Chapter 4

The growth rate of precipitates

4.1 Introduction

Calculating the diffusion-controlled growth rate is a problem which has received considerable attention, but for which solutions can still be classed in two categories. On the one hand, relatively complex mathematical approaches are used to solve the growth equation with as few assumptions as possible, or to account rigorously for the geometry of the growing particles, *etc.* (e.g. [89, 90, 91]). However, such approaches are difficult to use for practical purposes, as they often introduce quantities which are not known (for example, the cross-diffusion coefficients). On the other hand, solutions which are of practical interest rely on approximations which can be judged more or less important, but allow the calculations to be performed relatively easily and use parameters known for most materials (e.g. [92, 88, 93]).

In this work, an attempt is made to build as general a model as possible, while avoiding unnecessary approximations. For this reason, when possible, the diffusion coefficients of the components involved in the growth of the different precipitates found in austenitic stainless steels are calculated internally, and the use of MT-DATA removes the need for inputs such as the maximum volume fraction of a given phase, its composition, driving force, *etc.*

4.2 Calculation of the diffusion coefficients

4.2.a Calculation of the carbon diffusivity

As can be seen from the published literature [94], the diffusivity of carbon in austenite in the Fe-Cr-Ni-C system is strongly dependent on the composition. There are two main advantages in calculating the carbon diffusivity within the framework of any model created, rather than having it as an input. One is to considerably ease the task of the user who does not have to find a value in the literature for the particular composition being used. The other is that it may allow extrapolation to values which might not be found in the literature. The calculation of the carbon chemical diffusivity was done as suggested by Jönsson [94]. In his assessment of the carbon mobility in C-Cr-Fe-Ni alloys, Jönsson uses the multicomponent diffusion theory [95] and writes the chemical diffusivity of carbon, under the assumption that the concentration gradients of substitutional elements are negligible throughout the specimen, as:

$$\tilde{D}_C = RTy_{Va}M_C\Psi \tag{4.1}$$

where $\tilde{D}_C$ is the chemical diffusivity of carbon, y_{Va} the fraction of vacant sites on the interstitial sublattice, M_C the mobility of carbon, and Ψ the thermodynamic factor defined by:

$$\Psi = \frac{c_C}{RT}\frac{\partial \mu_C}{\partial c_C} \tag{4.2}$$

where C_C is the molar concentration of carbon. Jönsson then expresses the mobility M_C as:

$$M_C = M_\circ \exp\left(\frac{-Q_c}{RT}\right)\frac{1}{RT} = \frac{1}{RT}\exp\left(\frac{\Delta G_C^*}{RT}\right) \tag{4.3}$$

where $M_\circ$ is a frequency factor, Q_C an activation enthalpy and $\Delta G_C^* = RT\Phi_C - Q_C$, with Φ_C defined by $M_\circ = \exp(\Phi_C)$. Using the CALPHAD approach to model the composition dependency of the mobility, it is easier to fit the quantity ΔG_C^* than the frequency factor and activation enthalpy separately [94]. The quantity ΔG_C^* is therefore fitted using a sublattice model 4.4:

$$\Delta G_C^* = \sum_i \sum_j y_i y_j \Delta G_C^{*\,i:j}$$

$$+\sum_i \sum_{j>i} \sum_l y_i y_j y_l \left(\sum_r {}^r\Delta G_C^{*\,i,j:l} (y_i - y_j)^r \right)$$
$$+\sum_i \sum_l \sum_{m>l} y_i y_l y_m \left(\sum_r {}^r\Delta G_C^{*\,i:l,m} (y_l - y_m)^r \right) \qquad (4.4)$$

where the indices indicate which species occupies the different sublattices, separated by a colon, for example $\Delta G^{*\,Cr:Va}$ is for Cr on the first sublattice with nothing on the second (vacancy), $\Delta G^{*\,Fe,Cr:Va}$ is an interaction parameter for Fe and Cr on the first sublattice with nothing on the second. y_i is the fraction of the sites occupied by species i on its sublattice. If necessary, the individual parameters $\Delta G_C^{*\,i:j}$ are expressed as polynomials of the temperature.

Jönsson [94] provides the parameters for the mobility of carbon in austenite for Fe-Cr-Ni-C alloys, so that the influence of the Cr, Ni and C content on the diffusion coefficient of carbon in this phase can be calculated. These data have been used to calculate the diffusion coefficient of carbon within a FORTRAN (formula translation) program written to model the nucleation and growth of precipitates in austenitic stainless steels. The influence of other elements commonly found in such steels (e.g. Mo, Mn, Si, N, *etc.*) is only present as a modification of the site occupancy fractions for Fe, Cr, Ni and C, but there are no specific parameters. As is explained later, this FORTRAN program is interfaced with a library of subroutines which enable the use of MT-DATA internally. Therefore it is not a problem to calculate terms such as Ψ defined by equation 4.2. Typical calculated values are shown in table 4.1.

Material	NF709	AISI 304
$\tilde{D}_C$ / m^2 s^{-1}	4.87×10^{-13}	5.86×10^{-13}

Table 4.1: Typical calculated values for the chemical diffusivity of C in austenite at 1023 K, composition of these two steels can be found in table 1.1.

4.2.b The diffusivity of Fe, Cr and Ni

The same approach was used for Fe, Cr and Ni which allows diffusivity coefficient to be calculated within the program mentioned above, parameters were found in [36] and [96]. Table 4.2 shows examples of calculated diffusion coefficients for Cr, compared with values found in literature:

Material	Calculated	Literature
AISI 316 [97]	8.9×10^{-19} m^2 s^{-1}	6.2×10^{-19} m^2 s^{-1}
16Cr-14Ni [98]	5.54×10^{-19} m^2 s^{-1}	5.50×10^{-19} m^2 s^{-1}

Table 4.2: The diffusion coefficient of Cr in AISI 316 at 750 °C as calculated and found in different studies.

4.3 Calculation of the growth rate

The problem of calculating the growth rate is two-fold: firstly, it is necessary to be able to calculate the growth rate as a function of the supersaturation, that is as a function of the concentration profile at the interface. Secondly, it is necessary to determine the interface compositions which in turn fixes the supersaturation.

4.3.a Calculating the growth rate in a binary system

This section deals with the diffusion-controlled growth of a precipitate θ in a matrix γ, for a binary system. Under these conditions, the flux of solute in the matrix is given by:

$$J = -D\nabla c \tag{4.5}$$

where J is the flux of solute, D its diffusion coefficient in the matrix and c the molar or mass concentration, depending on the flux of interest. The growth rate ψ of θ is usually calculated by solving the diffusion equation, and equating the flux of solute to the amount incorporated into θ (figure 4.1 and equation 4.6):

$$\psi \left(c^{\theta\gamma} - c^{\gamma\theta} \right) = J \tag{4.6}$$

where $c^{\theta\gamma}$ is the concentration of solute in the precipitate in equilibrium with the matrix and $c^{\gamma\theta}$ the composition of the matrix in equilibrium with the precipitate. As is shown in figure 4.1, it is essential that the interface compositions are known in order to solve the problem. Under the assumption of local equilibrium, these are given by the equilibrium phase diagram. There are various effects which might cause a departure from local equilibrium, such as the effect of interface energy, the existence of stresses and the solute-drag effect (a review of these effects can be found in [99]). Much work has been dedicated to the treatment of multicomponent capillarity, which is presented in chapter 5. Other effects are assumed to be negligible.

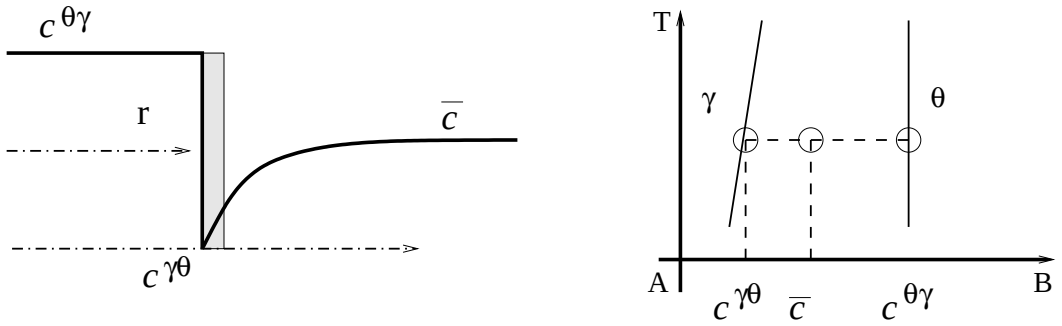

Figure 4.1: The concentration profile of the solute as a function of the distance from the interface matrix / precipitate. r is the coordinate of the interface between the matrix and the precipitate, $\overline{c}$ is the bulk alloy composition. The shaded area represents the amount of solute incorporated in the precipitate during a small amount of time. It must be equal to the amount of solute brought at the interface by the diffusion in the matrix.

For planar, cylindrical or spherical geometries, the growth rate can be generally expressed by [84]:

$$\psi = \frac{S\sqrt{D}}{2\sqrt{t}} \tag{4.7}$$

where ψ is the velocity of the interface, t is the time, and S is the solution of:

$$S^j = 2\ \Omega\ \frac{\exp(-\frac{S^2}{4})}{\Phi_j(S)} \tag{4.8}$$

where Ω, the supersaturation, is defined by $\Omega = (\overline{c} - c^{\gamma\theta})/(c^{\theta\gamma} - c^{\gamma\theta})$, and j is 1,2 or 3 depending on the geometry of the problem: planar, cylindrical and spherical respectively. $\Phi_j(S)$ is given by:

$$\Phi_j(S) = \int_S^\infty u^{1-j} \exp\left(-\frac{S^2}{4}\right) \mathrm{d}u \tag{4.9}$$

In cases where Ω is very close to 0 or very close to 1, asymptotic expansions can easily be found for the planar and spherical cases, by rewriting Φ using the erfc function and expanding the latter to the first terms of its equivalent series. The following results are obtained:

For small supersaturations ($\Omega \to 0$):

$$S^{\text{planar}} = \frac{2}{\sqrt{\pi}}\Omega \tag{4.10}$$

$$S^{\text{spherical}} = \sqrt{2\Omega} \tag{4.11}$$

For large supersaturations ($\Omega \to 1$):

$$S^{\text{planar}} = \sqrt{\left(\frac{2}{1-\Omega}\right)} \tag{4.12}$$

$$S^{\text{spherical}} = \sqrt{\left(\frac{6}{1-\Omega}\right)} \tag{4.13}$$

i Calculation of the exact solution

Although equation 4.8 can be solved using a FORTRAN program, this is not straightforward, particularly at large supersaturations, where the different terms have to be calculated in a carefully chosen order to avoid exceeding the limits of most computers. Instead,

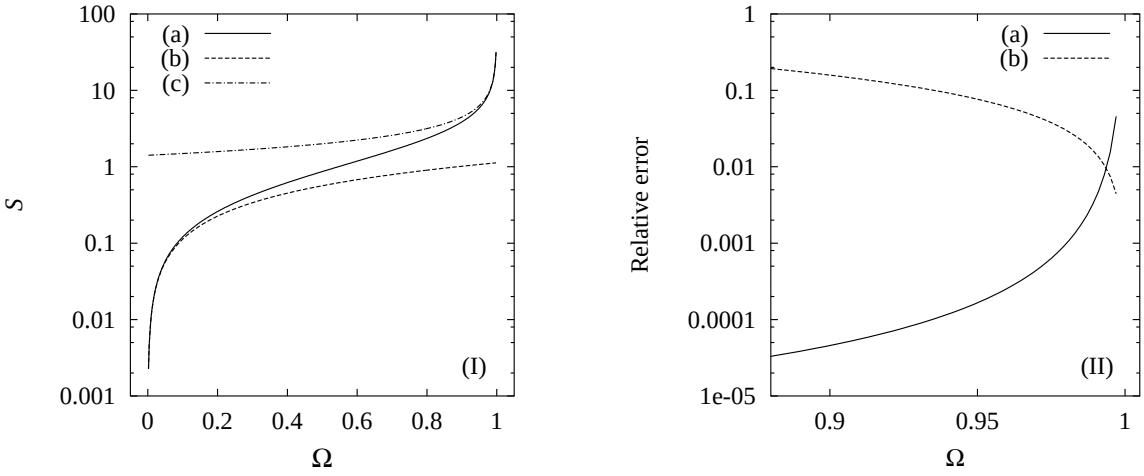

Figure 4.2: (I) The exact solution for the growth of a planar interface (a), and the approximations for small (b) and large (c) supersaturations. (II) The relative error (error due to method / exact solution) due to the use of equation 4.12 (a) and to the linear interpolation between calculated points (b).

a freely available mathematic package called SciLab (http://www-rocq.inria.fr/scilab/) was used to create a file containing the solutions for 500 points between 0 and 1. Intermediate values are found by linear interpolation. However, at large supersaturations, the error caused by this method becomes important. By comparing the relative error obtained by the linear interpolation and the use of the asymptotic expansions (figure 4.2), it was possible to optimise the use of one or another method as a function of the supersaturation.

As can be seen in figure 4.2, the relative error is always kept below 1% if the solution is calculated using equation 4.12 when $\Omega > 0.994$ while the linear interpolation between pre-calculated points gives a very reasonable error down to $\Omega = 0$. A similar method was used to calculate the growth rate of a spherical interface, and gave $\Omega = 0.990$ as the value above which it was preferable to use equation 4.13. A considerable calculation time is gained by this procedure, which almost reduces the calculation of S to a memory access.

4.3.b Calculation of the growth rate in a multicomponent alloy

The extension of the method described above is far from straightforward, as different effects appear in multicomponent systems, which, it is shown in this section, can not be reasonably neglected.

i The flux balance

The discussion that follows considers a ternary system as an example, but can be extended easily to a larger number of components.

Figure 4.3 illustrates the case of a ternary system in which a matrix γ is in equilibrium with a precipitate θ. The bulk composition corresponds to point P, and the equilibrium tie-line is that going through P. This tie-line defines diffusion profiles as illustrated, for which the supersaturations are all equal.

However, the elements involved often have very different diffusivities. For example, with Cr and C in austenite, the diffusion coefficients differ by a ratio of about about 10^6 at 750 °C. Therefore the concentration profiles defined by the mass-balance tie-line do not, in general, satisfy the following set of equations for a unique interface velocity ψ:

$$\begin{aligned} J_1 &= \psi \left(c_1^{\theta\gamma} - c_1^{\gamma\theta} \right) \\ J_2 &= \psi \left(c_2^{\theta\gamma} - c_2^{\gamma\theta} \right) \end{aligned} \tag{4.14}$$

or, taking the problem in the other sense, the diffusion profiles of the different elements, as fixed by the mass-balance tie-line, lead to different values of the interface velocity.

But there is no reason to select the equilibrium tie-line, that going through P, as the one defining the interface compositions. The mass-balance equations are no longer the determining constraints and must be replaced by equations 4.14. The tie-line fixed by these conditions will be referred to as the flux-balance tie-line.

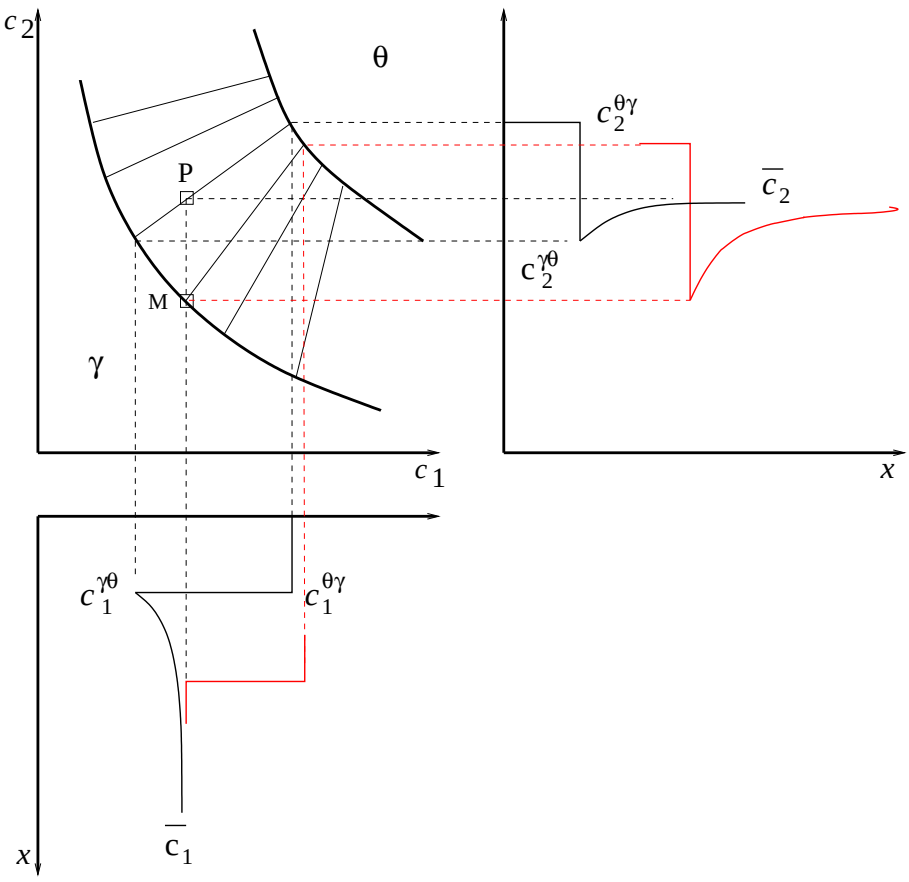

Figure 4.3: The flux-balance fixed tie-line going through M, can be quite different from the mass-balance fixed one, that passes through P, the bulk composition. In the case where 1 diffuses much faster than 2, its gradient may be strongly reduced.

ii The problem of identifying the flux-balance tie-line

Although the problem of identifying the flux-balance tie-line has received attention in a number of studies [89, 90], it remains, in practice, difficult to solve. If one is to account for this effect within a model describing the evolution of the precipitation, one needs to have access to the entire phase diagram for the phases concerned, and not, as is the case with binary system, just the interface compositions.

Earlier approaches by Fujita and Bhadeshia [93] have used simple analytical expressions to fit the phase boundary in the ternary system of interest. However, there are serious limitations to this method: first, the use of the model will be restricted to those systems for which the phase boundary have been fitted by a function, and second, the method is extremely difficult to extend to systems of more than three components.

The application interface of the thermodynamic calculation software MT-DATA [3] was used to provide an algorithm able to solve the problem in any system described in the SGTE (or any other) databases. It consists of a library of subroutines which can be called within a FORTRAN program to perform thermodynamic calculations with MT-DATA.

Before presenting the algorithm which was written to solve this problem in a general manner, it is necessary to look more carefully at the set of equations 4.14, and particularly at the fluxes. In multicomponent system, the flux of component i is related to the various concentration gradients according to:

$$J_i = -D_i \nabla c_i - \sum_{j \neq i} D_{ij} \nabla c_j \tag{4.15}$$

where the cross-diffusion terms ($D_{ij} \nabla c_j$) arise because the gradient of components other than i can modify its chemical potential. In the following, cross-diffusion terms have been neglected. Without this assumption, which is further discussed later, it is not possible to use equation 4.7.

4.3.c An algorithm to determine the tie-line satisfying the flux-balance

In this method, the velocity ψ_i (the index indicating which component profile is used) of the interface is calculated independently for each component composition profile, which implies that cross-diffusion terms in equation 4.15 are neglected. The aim is to find the tie-line for which all the ψ_i are identical. This is in fact reduced to equating the $S_i\sqrt{D_i}$, as shown by equation 4.7.

Figure 4.4 describes how the tie-line satisfying the flux-balance is identified in a pseudo-ternary system. Pseudo-ternary refers to a ternary sub-system of a multicomponent system. We consider here the example of the growth of $M_{23}C_6$. For the mass-balance tie-line, C and Cr have the same supersaturation ($\Omega_C = \Omega_{Cr}$), hence $S_C = S_{Cr}$. However C diffuses much faster than Cr, and therefore ψ_C, as calculated from the C concentration profile, will be much larger than ψ_{Cr}. The tie-line eventually giving $\psi_{Cr} = \psi_C$ considerably reduces Ω_C and increases Ω_{Cr}.

In systems with more than three components, this is repeated in a nested manner. For example, a first modification is done on Mo, which gives a new pseudo-ternary system in

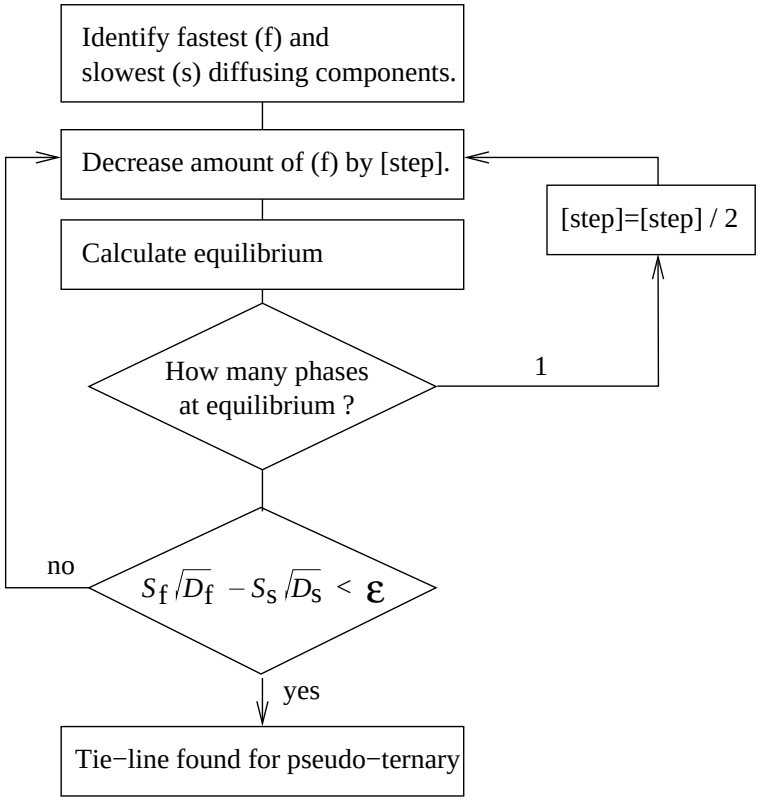

Figure 4.4: The algorithm written to find the tie-line satisfying the flux-balance in any system described in the databases used by MT-DATA; for each component the step is initially set to a tenth of its total amount.

which this algorithm is applied, to Cr and C. When the tie-line is found, the fluxes of Cr and C are identical, and need to be compared to that of Mo. The amount of Mo can then be corrected and the procedure repeated until the tie-line that gives identical fluxes for all elements involved is found.

This method is computer intensive, essentially because it is not possible to interact with MT-DATA on a low level and replace the mass balance constraint directly in the Gibbs energy optimisation process.

4.4 Overall kinetics

The overall kinetic is presented in chapter 6. For comparisons made later, it is however necessary to introduce the concept of soft-impingement.

When many precipitates form in the same matrix, whether they are of same or different nature, they compete for solute. To represent this, the mean-field approximation is used, in which the composition $\overline{c_i}$ is updated to reflect the amount of component i which has been incorporated during a time step by the various precipitates.

4.5 Consequences

4.5.a The growth rate

The growth rate calculated assuming that Cr and C control the process was found to be more than an order of magnitude larger than the one calculated assuming Cr control alone.

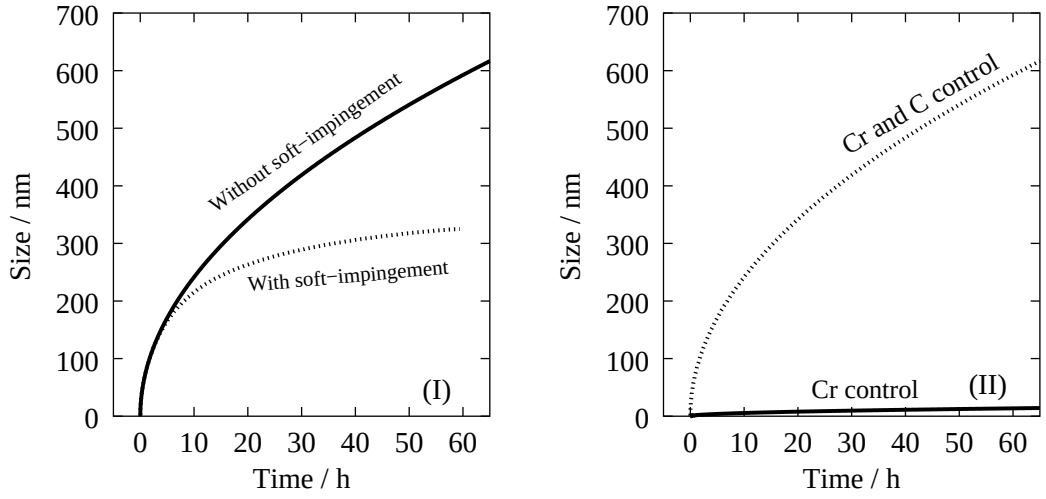

Figure 4.5: (I) Comparison between the calculated growth rates for $M_{23}C_6$ at 650 °C, in AISI 316 [97], with and without soft-impingement, under control of both Cr and C diffusion. (II) Comparison, without soft impingement, of the growth rate of a $M_{23}C_6$ particle nucleated at $t = 0$, at 650 °C, under Cr control alone, and Cr and C control.

Figure 4.5(I), shows the predicted radius of a $M_{23}C_6$ precipitate nucleated at $t = 0$, with and without accounting for soft impingement, which can have a strong effect on the growth rate. Since the purpose is here to compare the growth rates under different hypotheses and since the role of soft impingement is itself dependent on the growth rates, this effect has been removed to facilitate further comparisons. This means that

growth curves can only be representative of the real phenomenon at the early stages of the precipitation.

Figure 4.5(II) compares the growth rate under Cr and C diffusion control and under Cr diffusion control alone. In this situation, because of the very large difference between the diffusivity of carbon and chromium in austenite, the tie-line found to satisfy the flux-balance is virtually bringing the carbon gradient to zero (tie-line going through M in figure 4.3). As a consequence, at the early stages of precipitation, the composition of $M_{23}C_6$ and of the surrounding austenite, are expected to be fairly different from the equilibrium values.

4.5.b The composition of $M_{23}C_6$ in the Fe-Cr-Ni-C system

Several observations can be found which report an increasing Cr/Fe ratio during the growth of $M_{23}C_6$ (section 2.1.c). Table 4.3 shows the expected $M_{23}C_6$ composition at equilibrium, and the composition at the beginning of precipitation. As observed, the Cr/Fe ratio is much smaller at the onset of precipitation than for the equilibrium.

	Element	Fe	Cr	Mo	Mn
650 °C	Wt% (I)	4.7	64.61	9.95	0.001
	Wt% (II)	49.12	20.05	10.12	0.006
800 °C	Wt% (I)	7.9	62.37	9.03	0.005
	Wt% (II)	31.46	38.50	9.31	0.016

Table 4.3: The substitutional composition of $M_{23}C_6$ in two different cases: I is for the mass balance and II for the flux balance as calculated in this project. The steel composition was 17.5 Cr, 12.3 Ni, 2.5 Mo, 1.6 Mn, 0.07 C wt%, as in [97].

4.5.c Number of components accounted for

The number of components that can be accounted for in the calculation is firstly limited by the thermodynamic databases. Phases such as NbN, TiN and similar phases are modeled as pure substances in the SGTE databases, so that it is not possible to predict a change of composition, although, as explained in chapter 2, many works have reported variations in the composition and stoichiometry of these phases during growth.

In the case of $M_{23}C_6$, the elements Fe, Cr, Mo, Mn, Ni, and C can be included.

However, including minor elements such as Mo, Ni and Mn has little influence over the growth rate calculated with Cr and C diffusion, but greatly increases the computation time. For this reason, in the above calculations and following comparisons, only the diffusion of Cr and C have been used to calculate the growth rates.

4.6 Comparisons and discussions

Figure 4.6 shows the experimental results obtained by Záhumenský *et al.* [97] for a AISI 316 steel at 650 °C and 800 °C. As can be seen, the agreement is relatively poor since the experimental points lie in between the two curves corresponding to the Cr diffusion-controlled growth and the multicomponent growth (accounting for Cr and C diffusion). Furthermore, while the above method predicts a reduction of Cr/Fe well below 1 (40 Fe,

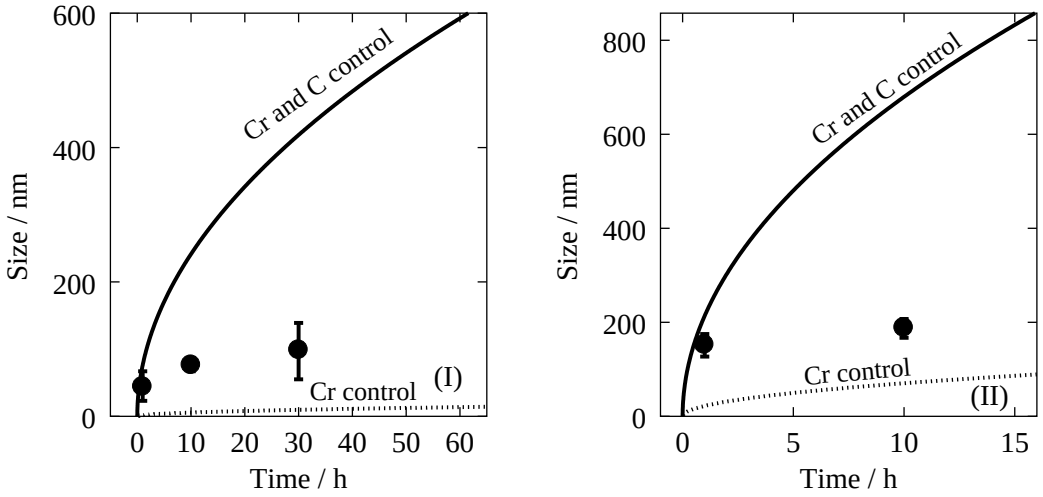

Figure 4.6: Comparison between predicted (lines) and measured (points) radii of $M_{23}C_6$ for the AISI 316 steel in [97], at (I) 650 °C and (II) 800 °C.

30 Cr wt%), the measurements made by Boeuf *et al.* [100] on an AISI 304 stainless steel report a Cr/Fe ratio slightly greater than 2 in the same conditions.

The overprediction of the radius can be partially attributed to the fact that soft-impingement is not accounted for. As shown in figure 4.5, soft-impingement flattens the growth curve considerably and quite early. But it appears that the difference is larger than could be attributed to this effect alone. Also, the absence of soft-impingement cannot explain why the compositions are different from the observations made by Boeuf *et al.*

As mentioned before, this method is based on the commonly used (e.g. [92, 88, 93]) assumption that the cross-diffusion terms in equation 4.15 are negligible, however, both the exaggerated growth rate and composition change indicate that this is not the case. Applying equation 4.15 to the example of $M_{23}C_6$, two fluxes have to be considered:

$$\begin{aligned} J_{\mathrm{C}} &= -D_{\mathrm{C}}\nabla c_{\mathrm{C}} - D_{\mathrm{CC}r}\nabla c_{\mathrm{C}r} \\ J_{\mathrm{C}r} &= -D_{\mathrm{C}r}\nabla c_{\mathrm{C}r} - D_{\mathrm{C}r\mathrm{C}}\nabla c_{\mathrm{C}} \end{aligned} \tag{4.16}$$

When the tie-line reaches point M in figure 4.3, the carbon gradient is almost reduced to zero, but there is a strong gradient of chromium concentration, so that even if $D_{\mathrm{CC}r} \ll D_{\mathrm{C}}$, it is not possible to conclude that $D_{\mathrm{CC}r}\nabla c_{\mathrm{C}r} \ll D_{\mathrm{C}}\nabla c_{\mathrm{C}}$ since $\nabla c_{\mathrm{C}r} \gg \nabla c_{\mathrm{C}}$.

Difficulties arising from the inclusion of cross-diffusion terms have been presented before. However, the following solution avoids this difficulty: in the most general formalism, it is a gradient of activity that drives diffusion. By reducing the gradient of carbon activity rather than its concentration gradient, it can be ensured that the carbon flux is really reaching a minimum. Furthermore, it can be considered, at this point, that the effect of the remaining carbon gradient on the activity of chromium is negligible, therefore allowing to identify $J_{\mathrm{C}r}$ to $-D_{\mathrm{C}r}\nabla c_{\mathrm{C}r}$. This means that the growth rate can be calculated by using the diffusion of chromium alone at the point where there is no carbon activity gradient. The following section describes the implementation of this method and the results obtained.

4.7 Improvement in the calculation of the flux-balance tie-line

Instead of reducing the carbon gradient and finding the tie-line which gives identical fluxes (under the assumption that cross-diffusion is negligible), the algorithm described in figure 4.4 was modified to find the interface composition for which the activity of carbon was equal to the far-field one. When this tie-line is found, the velocity of the interface is assumed to be that given by the diffusion of chromium.

As shown in figure 4.7 the agreement between the calculated and measured radii of $M_{23}C_6$ in AISI 316 is considerably improved. Without doubt, the overpredicted size of $M_{23}C_6$ after 10 h at 800 °C is due to the absence of soft-impingement, this temperature

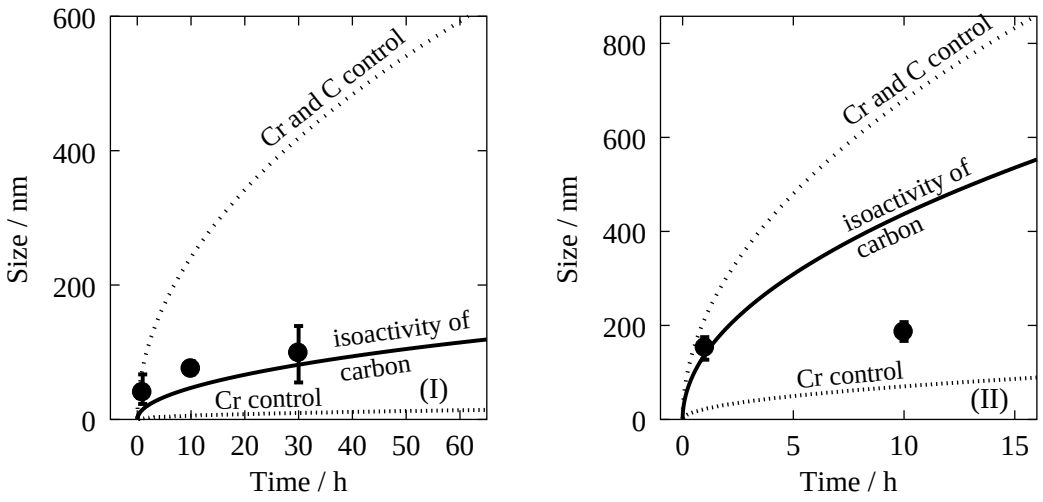

Figure 4.7: The radius of $M_{23}C_6$ at (I) 650 °C and (II) 800 °C. The agreement is best for the growth rate calculated with no gradient of carbon activity.

corresponding roughly to the nose of the TTT (time temperature transformation) curve for this category of steels [4], where the transformation is finished in a matter of hours.

The composition of $M_{23}C_6$ at the beginning of precipitation was calculated for the AISI 304 studied by Boeuf *et al.* [100]. Table 4.4 sumarises the observed initial Cr/Fe ratio and the calculated ones, using a zero gradient of carbon concentration and a zero gradient of carbon activity. The last method, which gives very satisfying predictions of the radius, also predicts well the Cr/Fe ratio.

	Cr/Fe ratio
Equilibrium	12
Boeuf *et al.* at $t = 0$	**2.1**
Flux balance	0.72
Carbon isoactivity	**2.2**

Table 4.4: The Cr/Fe ratio in $M_{23}C_6$ in different cases, for the AISI 304 steel studied by Boeuf *et al.*. The last method clearly gives satisfying agreement with experimental results.

4.8 Summary and conclusions

A FORTRAN program has been written, interfaced with the thermodynamic calculation software MT-DATA, to solve the problem of growth in multicomponent systems. It is shown that, although this approximation has been often used, neglecting the cross-diffusion terms is particularly inappropriate when trying to equate the fluxes, and lead to unrealistic results. A method has been proposed to solve the problem more rigorously without having to include such terms, by considering the activity of carbon. This last method predicts correctly not only the growth rate, but also the change in the $M_{23}C_6$ composition.